



## Oxygenated fraction and mass of organic aerosol from direct emission and atmospheric processing measured on the R/V *Ronald Brown* during TEXAQS/GoMACCS 2006

L. M. Russell,<sup>1</sup> S. Takahama,<sup>1</sup> S. Liu,<sup>1</sup> L. N. Hawkins,<sup>1</sup> D. S. Covert,<sup>2</sup> P. K. Quinn,<sup>3</sup> and T. S. Bates<sup>3</sup>

Received 10 October 2008; revised 24 January 2009; accepted 10 February 2009; published 4 April 2009.

[1] Submicron particles collected on Teflon filters aboard the R/V *Ronald Brown* during the Texas Air Quality Study and Gulf of Mexico Atmospheric Composition and Climate Study (TexAQS/GoMACCS) 2006 in and around the port of Houston, Texas, were measured by Fourier transform infrared (FTIR) and X-ray fluorescence for organic functional groups and elemental composition. Organic mass (OM) concentrations ( $1\text{--}25\ \mu\text{g m}^{-3}$ ) for ambient particle samples measured by FTIR showed good agreement with measurements made with an aerosol mass spectrometer. The fractions of organic mass identified as alkane and carboxylic acid groups were 47% and 32%, respectively. Three different types of air masses were identified on the basis of the air mass origin and the radon concentration, with significantly higher carboxylic acid group mass fractions in air masses from the north (35%) than the south (29%) or Gulf of Mexico (26%). Positive matrix factorization analysis attributed carboxylic acid fractions of 30–35% to factors with mild or strong correlations ( $r > 0.5$ ) to elemental signatures of oil combustion and 9–24% to wood smoke, indicating that part of the carboxylic acid fraction of OM was formed by the same sources that controlled the metal emissions, namely the oil and wood combustion activities. The implication is that a substantial part of the measured carboxylic acid contribution was formed independently of traditionally “secondary” processes, which would be affected by atmospheric (both photochemical and meteorological) conditions and other emission sources. The carboxylic acid group fractions in the Gulf of Mexico and south air masses (GAM and SAM, respectively) were largely oil combustion emissions from ships as well as background marine sources, with only limited recent land influences (based on radon concentrations). Alcohol groups accounted for 14% of OM (mostly associated with oil combustion emissions and background sources), and amine groups accounted for 4% of OM in all air masses. Organosulfate groups were found in GAM and SAM, accounting for 1% and 3% of OM, respectively. Two thirds of the OM and oxygen-to-carbon (O/C) measured could be attributed to oil and wood combustion sources on the basis of mild or strong correlations to coemitted, nonvolatile trace metals, with the remaining one third being associated with atmospherically processed organic aerosol. The cloud condensation nuclei (CCN) fraction (normalized by total condensation nuclei) had weak correlations to the alcohol and amine group fractions and mild correlation with O/C, also varying inversely with alkane group fraction. The chemical components that influenced  $f(\text{RH})$  were sulfate, organic, and nitrate fraction, but this contrast is consistent with the size-distribution dependence of CCN counters and nephelometers.

**Citation:** Russell, L. M., S. Takahama, S. Liu, L. N. Hawkins, D. S. Covert, P. K. Quinn, and T. S. Bates (2009), Oxygenated fraction and mass of organic aerosol from direct emission and atmospheric processing measured on the R/V *Ronald Brown* during TEXAQS/GoMACCS 2006, *J. Geophys. Res.*, *114*, D00F05, doi:10.1029/2008JD011275.

<sup>1</sup>Scripps Institution of Oceanography, University of California, San Diego, La Jolla, California, USA.

<sup>2</sup>Joint Institute for the Study of the Atmospheres and Oceans, University of Washington, Seattle, Washington, USA.

<sup>3</sup>Pacific Marine Environmental Laboratory, National Oceanic and Atmospheric Administration, Seattle, Washington, USA.

### 1. Background

[2] The organic fraction of aerosol particles accounts for significant mass in both polluted and unpolluted areas of the lower troposphere [McMurry *et al.*, 2003; Zhang *et al.*, 2007; Kanakidou *et al.*, 2005]. Like other types of aerosol particles, multiple natural and man-made sources contribute

to emissions of organic particles [Simoneit *et al.*, 2004; Kanakidou *et al.*, 2005; Decesari *et al.*, 2007]. Unlike sulfate, nitrate, and ammonium components in aerosols, the organic fraction consists of an extraordinary variety of organic molecules and mixtures. To date, neither the sources nor the ambient mixtures have been quantitatively characterized, as a result of the significant complexity of molecular speciation in small samples. Consequently, the uncertainties associated with the reactions, phase changes, lifetimes, and fates of organic components in the atmosphere remain large [Turpin *et al.*, 2000].

[3] An important question for both atmospheric chemistry and environmental regulations is posed as what fractions of the organic carbon mass and its associated oxygenated groups are formed at the source (“primary”) or in the atmosphere (“secondary”). Since this distinction is challenging to measure in the atmosphere, another approach is to distinguish between organic components formed directly from the emissions of one source type (“emitted”) from those formed by multiple sources or by a set of atmospheric (including both photochemical and meteorological) conditions (“processed”). This alternative approach to classifying organic aerosol is benefited by a clear operational definition for atmospheric measurements, as the emitted organic components are mildly or strongly correlated to trace metals (or other nonprocessed source emissions) and the processed organic components will vary with atmospheric composition and conditions (including sunlight, relative humidity, and oxidant concentrations). This definition is based on a statistical correlation with nonvolatile trace metals (which are found in primary particles) rather than the historical criterion of the phase of the organic components themselves at emission, but it provides a useful regulatory application by separating the organic components associated with a single source type from those dependent on other atmospheric pollutants that may be caused by multiple sources or conditions. Both “emitted” and “processed” organics will include oxygenated organic compounds; the division is between those oxygenated organic compounds that form sufficiently rapidly that their formation is independent of time since emission and ambient oxidant concentrations (i.e., they essentially “always” form from this source, resulting in a mild or strong correlation to other source emissions) and those compounds for which other atmospheric variables dominate. The other variables may result from time delays associated with slow oxidation processes (“aging”) or with the need for high oxidant concentrations (which may have resulted from high volatile organic compound, VOC, or NO<sub>x</sub> emissions from other sources).

[4] An important related question is how the organic compounds from these different types of sources affect particle behavior in the atmosphere. Three types of measurements have been used to investigate the water uptake properties of organic particles: one determining their ability to nucleate cloud droplets (cloud condensation nuclei or CCN), one measuring the optical hygroscopicity ( $f(RH)$ ), and one using their solubility (water-soluble organic carbon or WSOC). Recent work has suggested or assumed correlations between one or more of these hygroscopicity metrics and the oxygenated fraction of organics [Ming and Russell, 2001; Maria and Russell, 2005; Topping *et al.*, 2005;

*Ervens et al.*, 2005; Kondo *et al.*, 2007 Quinn *et al.*, 2007; Shilling *et al.*, 2007]. In practice, each of these metrics quantifies a specific aspect of water uptake which also depends on the chemical mixtures in the particles: (1) CCN measures water uptake at low (atmospherically relevant) supersaturations, reflecting the hygroscopicity and surface tension of the particle mixture for the minimum water needed for activation; (2)  $f(RH)$  measures increases in scattering at subsaturated relative humidities, indicating hygroscopicity and optical scattering in noncloudy conditions; and (3) WSOC measures soluble components that activate at high supersaturations, reflecting the mixture and the component solubility in highly diluted aqueous solutions. While each of these water-uptake properties depends in part on the polarity of the organic components in the mixture (which are expected to increase with the oxygenated fraction of organics), each of them also depends on other physical properties including the size of the ambient and sampled particles by each technique.

[5] In this work, we show that the chemical components controlling these three types of water uptake can be very distinct by analyzing measurements of organic functional groups and inorganic components. This characterization also provides a step toward linking organic mixtures in particles to the sources that emit them. The functional-group quantification of organic components is approximate, but the identification of different bond types provides features of organic mixtures that can be compared to simultaneous measurements of trace metals. The unique trace metal signatures of some sources are well correlated to associated fractions of the organic functional groups with known emission sources. The measurements in this work were collected during a 30-day period aboard a ship traveling near Houston, Texas, with high ambient temperatures and relative humidity, using fixed-temperature, humidity, and size-cut sampling protocols [Quinn *et al.*, 2007; Bates *et al.*, 2008].

## 2. Introduction

[6] Using the Texas Air Quality Study and Gulf of Mexico Atmospheric Composition and Climate Study (TexAQS/GoMACCS) 2006 measurements in Houston, Bates *et al.* [2008] have identified three air mass types on the basis of radon concentrations and back trajectories: southerly flow from the Gulf of Mexico with negligible concentrations of radon indicating little time spent over land (Gulf air masses (GAM)), southerly flow from the Gulf of Mexico polluted by nearby land-based sources and small radon concentrations (south air masses (SAM)), and northerly flow which had traveled over land for four or more days with high radon concentrations indicating significant time spent over land (north air masses (NAM)). Their work showed that the NAM had higher concentrations of  $m/z$  44 fragments, associated with more oxygenated organic compounds [Zhang *et al.*, 2005; Takegawa *et al.*, 2007]. The less oxygenated (or hydrocarbon-like organic aerosol, HOA) organic fraction associated with  $m/z$  57 fragments was associated mostly with smaller particles (<500 nm). Their work suggested that the NAM included a mixture of organics that were probably emitted during the course of

several days prior to sampling resulting in more time for photochemical aging.

[7] In this work, we evaluate the organic functional group composition associated with these same three air mass types in order to characterize more specifically the differences in the organic composition of the NAM relative to the GAM and SAM. Our work confirms the difference noted in the aerosol mass spectrometer (AMS) measurements of organic mass fragments using an independent, chemical-bond based technique (Fourier transform infrared, or FTIR) and goes on to show that this oxidized fraction was associated with carboxylic acid and alcohol groups. In addition, we have employed correlations of the individual organic functional groups to concentrations of trace metals to distinguish some general classes of sources using positive matrix factorization (PMF) [Paatero and Tapper, 1994]. The resulting PMF factors provide a framework that separates the organic mass and functional groups into separate fractions that are based on their sources. While there are large uncertainties in emissions, mixing, and oxidants that limit this analysis to only a few very gross types of different sources, this work illustrates important differences in the characteristics of the organic mixtures from oil combustion, wood smoke, and atmospherically processed sources in the GAM, SAM, and NAM.

### 3. Methods (Organic and Elemental Measurements of Submicron Particles)

[8] Submicron particles were sampled from a humidity- and temperature-controlled isokinetic inlet in parallel with filters collected for extraction and ionic analysis [Quinn *et al.*, 2007; Bates *et al.*, 2008]. Teflon filters were used as substrates and showed negligible adsorption of volatile organic compounds (VOCs) on duplicate back filters collected simultaneously with each sample [Maria *et al.*, 2003; Gilardoni *et al.*, 2007]. The back filters provide a measure of adsorption during sampling and contamination during handling (loading and unloading) and storage. Organic components collected on each back filter were analyzed as a measure of sampling error. Parallel sampling through a single 1- $\mu\text{m}$  sharp-cut cyclone (SCC 2.229PM1, BGI Inc., Waltham, Massachusetts) was used to collect simultaneous short (6 to 14 h) and long (24 h) samples for a total of 112 samples. Simultaneous samples were used to check for sampling consistency by comparing summed short to long samples, and long samples were used to check for groups present at low concentrations that fell below detection limit in the shorter samples.

[9] Each sample (and associated back filter) was nondestructively analyzed by transmission FTIR. FTIR measurements of absorbance characterized the functional groups associated with major carbon bond types, including saturated aliphatic (alkane) groups, unsaturated aliphatic (alkene) groups, aromatic groups, alcohol (used here to include phenol and polyol) groups, carboxylic acid groups, non-acidic carbonyl groups, primary amine groups, and organosulfate groups. The spectra were interpreted using an automated algorithm to perform baselining, peak-fitting, and integration with a revised version of the approach described previously [Maria *et al.*, 2002, 2003, 2004; Maria and Russell, 2005], using calibrations revised for the Tensor

27 spectrometer with RT-DLATGS detector (Bruker Optics, Ettlingen, Germany) [Gilardoni *et al.*, 2007]. For this new algorithm, additional calibrations of amines and carboxylic acids were used to improve accuracy by quantifying additional peaks at 2625  $\text{cm}^{-1}$  and 2600–2800  $\text{cm}^{-1}$ . The revised algorithm is tuned to quantify ambient aerosol concentrations as specified in auxiliary material Text S1 and Table S1.<sup>1</sup> Complete sets of internal standards for organic components of the atmosphere are not available, in part because the ambient particle composition is not fully known. In addition, the complexity of ambient mixtures of organic compounds in the atmosphere results in mixtures that cannot be fully resolved by FTIR. All of the measured functional groups are summed to calculate organic mass (OM). Estimates of the accuracy, errors, and detection limits of this technique for ambient measurements are discussed by Russell [2003].

[10] X-ray fluorescence (XRF) measurements were conducted by Chester LabNet (Tigard, Oregon) on the same filters used for FTIR to provide trace metal concentrations for elements heavier than Na [Maria *et al.*, 2003]. Elemental concentrations were above detection for 30% to 100% of the ambient samples collected. Twenty-eight of the 112 filters measured had spectra with detectable absorbance at 876  $\text{cm}^{-1}$ , where organosulfate, carbonate, and bisulfate absorb. After XRF analysis, these 28 filters were rinsed with hexane and acetone to separate organosulfate groups from bisulfate and carbonate; 22 of these samples had concentrations of organosulfate above the detection limit.

[11] Quadrupole Aerosol Mass Spectrometer (AMS, Aerodyne Inc., Billerica, Massachusetts) measurements were used to make real time measurements of nonrefractory organic and ionic mass fragments, as summarized by Bates *et al.* [2008]. In addition to the standard calibrations for AMS OM measurements [Jayne *et al.*, 2000; Jimenez *et al.*, 2003; Allan *et al.*, 2003], onboard intercomparisons of the multiple organic methods were carried out using mixtures of sucrose and ammonium sulfate. FTIR spectra of these sampled mixtures were consistent with the presence of alcohol and alkane groups (similar to those expected for sucrose) as well as ammonium ions.

[12] Measurements of cloud condensation nuclei (CCN, Droplet Measurement Technologies, Boulder, Colorado) at 0.44% supersaturation are described by Quinn *et al.* [2007]. A particle-into-liquid-sampler (PILS) was used to collect a fraction of the submicron organic particles in a distilled water stream for total carbon analysis [Weber *et al.*, 2001; Orsini *et al.*, 2003; Sorooshian *et al.*, 2006]. This method has been shown to collect refractory and nonrefractory organic compounds that are dissolved by excess water in filter extraction with known water quantities [e.g., Miyazaki *et al.*, 2007] and is referred to here as water soluble organic carbon (WSOC). The optical hygroscopic growth factor of the submicron aerosol was measured from the particulate light scattering coefficient ( $\sigma_{\text{sp}}$ ) using two three-wavelength nephelometers (Model 3563, TSI Inc., St Paul, Minnesota), with one nephelometer operated at 25% relative humidity (RH) using diffusion drying and the other operated at 82 to 87% RH using water vapor addition. Both nephelometers

<sup>1</sup>Auxiliary material data sets are available at <ftp://ftp.agu.org/apend/jd/2008/jd011275>. Other auxiliary material files are in the HTML.

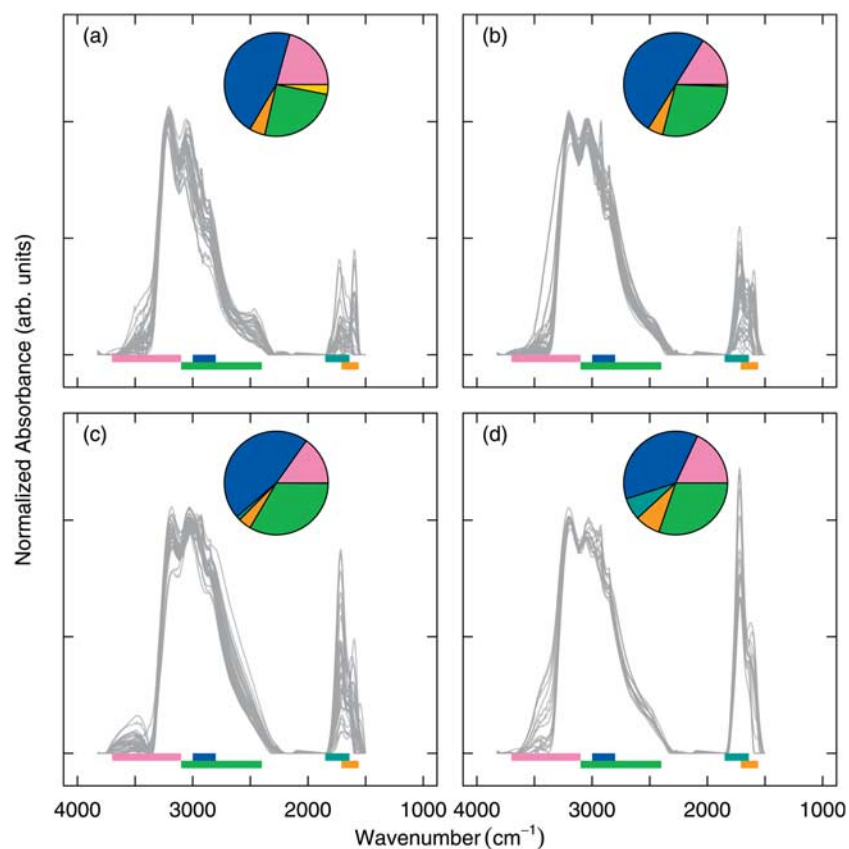


**Figure 1.** FTIR spectra during TexAQS/GoMACCS '06 from (a) cluster category S1, (b) cluster category S2, (c) cluster category N1, and (d) cluster category N2. Horizontal bars represent regions of absorbance: alcohol (hot pink), alkane (blue), carbonyl (teal), amine (orange), acid (green), organosulfur (yellow; not shown in spectra); pie chart shows relative contributions of functional group in each cluster (organosulfate is not shown as it is below the range displayed, 1500–3500  $\text{cm}^{-1}$ ).

were operated at 27°C. The optical hygroscopic growth factor is defined as

$$f(\text{RH}) = \sigma_{\text{sp}}(85\% \text{RH}) / \sigma_{\text{sp}}(25\% \text{RH}).$$

The value of  $\sigma_{\text{sp}}(85\% \text{RH})$  was determined from the measured high-RH scattering coefficient by the Kasten formula [Carrico *et al.*, 2000; Kaku *et al.*, 2006].

#### 4. Results

[13] Normalized FTIR spectra from all ambient samples collected during the project are shown in Figure 1, where they have been grouped according to a Ward cluster analysis to identify similarities among the measured organic spectra. Measured concentrations of organic mass varied from less than 1  $\mu\text{g m}^{-3}$  in GAM to more than 20  $\mu\text{g m}^{-3}$  in NAM, with the project mean and standard deviation listed in Table 1 at a concentration of  $4.7 \pm 3.9 \mu\text{g m}^{-3}$ . The functional group composition is shown in Figure 2 for the August and September 2006 measurement campaign. On average, the composition was largely alkane groups (47%), with carboxylic acid and alcohol groups accounting for approximately 32% and 14%, respectively. Amine groups made up almost 4% of average composition, and nonacid

carbonyl groups, when above detection limits, accounted for 1%.

[14] Organosulfate groups in 22 samples contributed 1% of the OM. None of the filters contained alkene or aromatic groups at loadings above the detection limit (as described in auxiliary material Text S1 and Table S1), corresponding to concentrations that were approximately 1.1% and 1.4% of OM, respectively. The FTIR and XRF data reported here are available at [http://saga.pmel.noaa.gov/Field/TEXAQS/post\\_cruise\\_data/](http://saga.pmel.noaa.gov/Field/TEXAQS/post_cruise_data/).

[15] The trace metal composition from XRF included only one element that averaged more than 100  $\text{ng m}^{-3}$  (S) and seven (Na, Al, Si, K, Ca, Fe) that exceeded 10  $\text{ng m}^{-3}$ . The remaining measured crustal and combustion metals were present in concentrations between 1 and 10  $\text{ng m}^{-3}$  (Ti, V, Ni, Zn, Sn), between 0.1 and 1  $\text{ng m}^{-3}$  (Cr, Mn, Cu, As, Br, Pb). Mg, P, Cl, Co, Cu, Ga, Ge, Rb, Sr, Y, Zr, Mo, Pd, Ag, Cd, In, Sb, Ba, La, and Hg were below detection in more than 70% of the samples, and average concentrations are not reported.

#### 4.1. FTIR/AMS Comparisons of OM, O/C, and Organic Functional Groups

[16] FTIR measurements of OM as the sum of all measured organic functional groups have typically compared well with other measurements of total organic carbon and

**Table 1.** Mean and Standard Deviation of Measured OM, Organic Functional Group, OM/OC, O/C, m/z 44, OOA, HOA, WSOC, and Elemental Concentrations for TexAQS/GoMACCS and for Periods With GAM, SAM, and NAM Measured by FTIR, AMS, PILS, and XRF<sup>a</sup>

	TexAQS/GoMACCS '06	GAM	SAM	NAM
FTIR OM ( $\mu\text{g m}^{-3}$ )	4.9 $\pm$ 4.1	2.1 $\pm$ 1.0	3.6 $\pm$ 1.9	9.0 $\pm$ 4.7
AMS OM ( $\mu\text{g m}^{-3}$ )	4.3 $\pm$ 5.1	0.77 $\pm$ 1.5	2.6 $\pm$ 1.7	9.7 $\pm$ 5.6
WSOC ( $\mu\text{g m}^{-3}$ )	1.2 $\pm$ 1.3	0.17 $\pm$ 0.36	0.74 $\pm$ 0.40	2.6 $\pm$ 1.4
FTIR organic functional groups ( $\mu\text{g m}^{-3}$ )				
Alkane	2.2 $\pm$ 1.9 (46%)	0.97 $\pm$ 0.55 (46%)	1.8 $\pm$ 1.0 (51%)	3.9 $\pm$ 2.3 (43%)
Carboxylic acid	1.5 $\pm$ 1.4 (31%)	0.52 $\pm$ 0.27 (25%)	1.0 $\pm$ 0.55 (28%)	3.0 $\pm$ 1.7 (33%)
Alcohol	0.82 $\pm$ 0.68 (17%)	0.45 $\pm$ 0.24 (22%)	0.56 $\pm$ 0.40 (16%)	1.5 $\pm$ 0.77 (16%)
Amine	0.25 $\pm$ 0.26 (5%)	0.10 $\pm$ 0.070 (5%)	0.16 $\pm$ 0.13 (4%)	0.48 $\pm$ 0.33 (5%)
Nonacid Carbonyl	0.070 $\pm$ 0.27 (1%)	0.0 $\pm$ 0.0 (0%)	0.0 $\pm$ 0.0 (0%)	0.23 $\pm$ 0.43 (3%)
Organosulfates	0.030 $\pm$ 0.090 (1%)	0.060 $\pm$ 0.090 (3%)	0.04 $\pm$ 0.13 (1%)	0.0 $\pm$ 0.0 (0%)
FTIR OM/OC (mass)	1.8 $\pm$ 0.14	1.8 $\pm$ 0.19	1.7 $\pm$ 0.10	1.8 $\pm$ 0.11
FTIR O/C (atomic)	0.41 $\pm$ 0.090	0.43 $\pm$ 0.11	0.37 $\pm$ 0.060	0.46 $\pm$ 0.080
AMS m/z 44 fraction (mass)	0.13 $\pm$ 0.04	0.16 $\pm$ 0.03	0.10 $\pm$ 0.03	0.15 $\pm$ 0.02
AMS OOA ( $\mu\text{g m}^{-3}$ )	3.2 $\pm$ 4.0	0.98 $\pm$ 1.9	1.3 $\pm$ 1.3	7.4 $\pm$ 4.2
AMS HOA ( $\mu\text{g m}^{-3}$ )	1.0 $\pm$ 1.2	0.12 $\pm$ 0.12	1.0 $\pm$ 0.67	1.8 $\pm$ 1.6
XRF elements ( $\text{ng m}^{-3}$ )				
Na	40 $\pm$ 23	29 $\pm$ 19	50 $\pm$ 21	33 $\pm$ 23
Al	44 $\pm$ 66	45 $\pm$ 63	41 $\pm$ 38	29 $\pm$ 46
Si	99 $\pm$ 150	87 $\pm$ 130	97 $\pm$ 92	64 $\pm$ 110
S	950 $\pm$ 690	600 $\pm$ 240	870 $\pm$ 380	1700 $\pm$ 1100
K	25 $\pm$ 19	16 $\pm$ 15	20 $\pm$ 9.9	41 $\pm$ 19
Ca	17 $\pm$ 15	13 $\pm$ 13	18 $\pm$ 8.8	15 $\pm$ 11
Ti	3.0 $\pm$ 4.9	2.7 $\pm$ 4.1	3.0 $\pm$ 3.9	1.9 $\pm$ 3.2
V	13 $\pm$ 27	3.7 $\pm$ 2.3	23 $\pm$ 40	9.4 $\pm$ 6.9
Cr	0.53 $\pm$ 0.81	0.50 $\pm$ 0.94	0.44 $\pm$ 0.72	0.93 $\pm$ 1.0
Mn	0.56 $\pm$ 1.11	0.17 $\pm$ 0.51	0.54 $\pm$ 1.1	1.1 $\pm$ 1.6
Fe	32 $\pm$ 39	24 $\pm$ 31	30 $\pm$ 24	33 $\pm$ 32
Ni	4.1 $\pm$ 7.3	1.6 $\pm$ 1.1	6.9 $\pm$ 11	3.2 $\pm$ 3.0
Zn	4.7 $\pm$ 7.4	1.1 $\pm$ 1.1	3.2 $\pm$ 2.4	14 $\pm$ 13
As	0.38 $\pm$ 0.46	0.17 $\pm$ 0.25	0.44 $\pm$ 0.50	0.65 $\pm$ 0.57
Se	0.17 $\pm$ 0.33	0.040 $\pm$ 0.060	0.090 $\pm$ 0.13	0.54 $\pm$ 0.58
Br	0.98 $\pm$ 1.1	0.25 $\pm$ 0.30	0.76 $\pm$ 0.59	2.4 $\pm$ 1.6
Sn	9.3 $\pm$ 5.8	10 $\pm$ 7.6	8.4 $\pm$ 4.6	11 $\pm$ 4.5
Pb	0.73 $\pm$ 0.98	0.26 $\pm$ 0.34	0.67 $\pm$ 0.72	1.7 $\pm$ 1.6

<sup>a</sup>FTIR and XRF concentrations are shown for elements with less than 70% of the values below the detection limit. (The numbers in parentheses are the percentages of the functional group masses to OM.)

mass concentrations for simultaneous and collocated samples, within the expected uncertainties of each technique [Maria *et al.*, 2002, 2003; Gilardoni *et al.*, 2007]. Figure 3 shows that at low concentrations the FTIR OM frequently exceeds the AMS OM, but in general the AMS and FTIR OM agree well. The slope of the sum of the measured FTIR functional groups for samples shorter than 14 h with AMS OM averaged to these sampling times is 1.06 with a strong correlation coefficient of  $r = 0.84$ , which is within the agreement expected of  $\pm 20\%$ . The 24-h samples taken as duplicates are omitted in calculating the line fit as the probability of evaporation losses of OM is higher [Mader and Pankow, 2001]. The differences in the scatter between the AMS and FTIR samples may result from some minor evaporation in sample collection in short samples, from errors in the correction for particles larger than 550 nm that have low transmission efficiency in the AMS but are captured by the 1- $\mu\text{m}$  cyclone (1.0  $\mu\text{m}$  50% aerodynamic cutoff diameter) upstream of the FTIR filters, from transparent or hidden organic components that cannot be resolved in the FTIR spectra (e.g., peroxides, tertiary carbons), from composition-dependent collection efficiencies that are not accounted for in the AMS, and other method limitations [Russell, 2003; Quinn *et al.*, 2006].

[17] The oxygen in the oxygen-containing organic functional groups can be summed and normalized by the carbon in all measured organic groups to estimate atomic (organic) O/C from FTIR measurements. O/C has been estimated from quadrupole AMS measurements by scaling the mass fraction of m/z 44 fragments to the total organic mass fragments and comparing to high-resolution AMS measurements [Aiken *et al.*, 2008; Shilling *et al.*, 2008]. For the TexAQS/GoMACCS samples, the mean FTIR O/C was 0.46 with a range of 0.3–0.9 during the project, and the AMS m/z 44 mass fraction mean was 13% with a range of 5 to 21% with the corresponding O/C being 0.3–0.9 [Aiken *et al.*, 2008]. The scatter of FTIR O/C to AMS m/z 44 mass fraction is large with a Pearson's coefficient of 0.36, but most of the values fall between the two proposed relationships of O/C to m/z 44 mass fraction [Aiken *et al.*, 2008; Shilling *et al.*, 2008]. A difference of 0.1 O/C is equivalent to 5% of the O/C expected for carboxylic acid groups (O/C = 2) or 10% of a 1:1 mixture of alkane and carboxylic acid groups (O/C = 1), making the discrepancies within the uncertainties of both FTIR and AMS. The poor correlation reflects partly the limited number and small dynamic range of measurements (with most of the measured values between 0.3 and 0.9). However, Figure 4 shows that many of

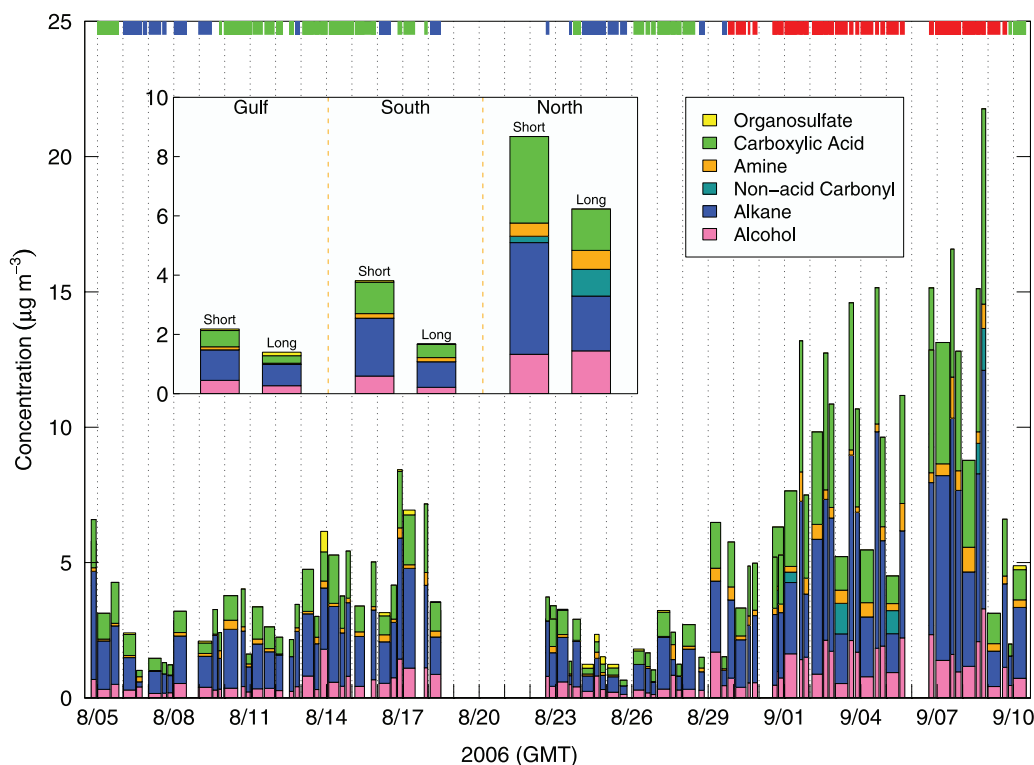


**Figure 2.** Time series of OM and organic functional groups as stacked bars (with same color scheme as in Figure 1) measured by FTIR during short (6 to 14 h) samples with GAM (blue), SAM (green), and NAM (red) marked by top colored bars. The inset shows the lower OM and organic functional groups associated with the long ( $\sim 24$  h) samples relative to the short samples.

the FTIR values are lower than the *Aiken et al.* [2008] ambient relationship for  $m/z$  44 mass fraction.

[18] The lower FTIR O/C results in part from using the quadrupole AMS-based estimate which may omit the contribution of amines to the total carbon. The values where FTIR O/C compares well with the *Aiken et al.* [2008] and *Shilling et al.* [2008] parameterizations typically include compositions with very high (0.3) mass fractions of carboxylic acid groups, suggesting that some of the scatter in the comparison is associated with the way in which nonacid oxygen-containing organic groups (e.g., peroxy groups which are omitted by FTIR) are measured in these two approaches. Omitting the high alcohol ( $>0.2$ ) and high organosulfate ( $>0.1$ ) group mass fraction measurements, the remaining O/C for only the higher acid fraction measurements has  $r = 0.42$ , slope of 0.017, and intercept at 0.20 (which provide a parameterization slightly lower than the slope of 0.022 and intercept of 0.17 found for smog chamber measurements by *Shilling et al.* [2008]). All three of the measured relationships between measured O/C and  $m/z$ 44 mass fraction are lower than pure laboratory reference standards [*Alfarra, 2004*], suggesting that some differences may reflect differences in the fragmentation of different acid compounds.

[19] Organic and inorganic components are frequently coemitted by urban sources, resulting in correlations in their observed atmospheric concentrations [*Gilardoni et al., 2007; Kondo et al., 2007; Bates et al., 2008*]. To show a chemical relationship between components or properties, we have reviewed the behavior of component concentra-

tions normalized by the relevant total concentration. Carboxylic acids are expected to have a high correlation to  $m/z$  44 mass fraction [*Alfarra, 2004*]. The carboxylic acid group mass fractions have very little correlation ( $r =$

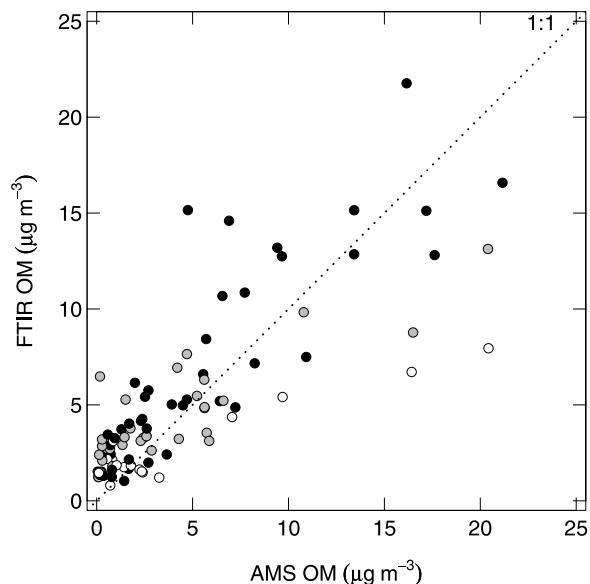


**Figure 3.** Comparison of OM measured by FTIR and AMS. The fill color for the circle markers indicates FTIR sample duration of less than 8 h (black), 8 to 14 h (gray), and 14 to 24 h (white).

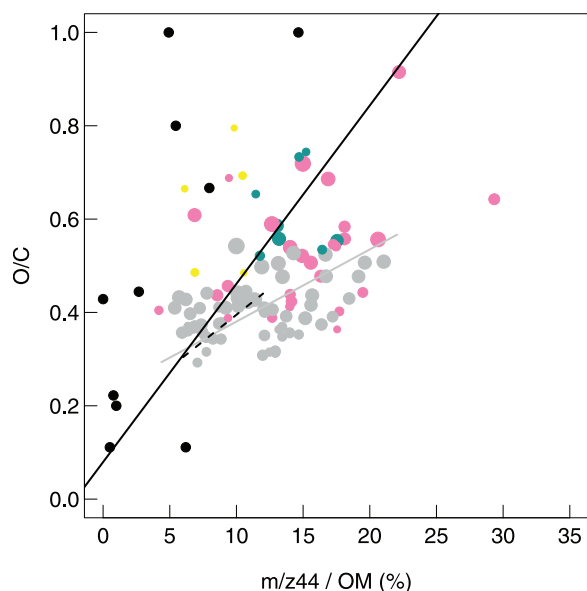


**Figure 4.** Comparison of O/C measured by FTIR with AMS  $m/z$  44 mass fraction showing estimated submicron  $m/z$  44 mass fraction (circles). Colored markers indicate measurements with O/C from groups other than acid: alcohol (pink) O/C > 0.15, organosulfate (yellow) O/C > 0.05, and nonacidic carbonyl (teal) O/C > 0.05. Grey line indicates the fit to only the gray markers and has intercept 0.19 and slope 0.017. Marker size increases with carboxylic acid group mass fraction. Black lines show correlations of O/C to AMS  $m/z$  44 mass fraction from Aiken *et al.* [2008] (solid line) and Shilling *et al.* [2008] (dotted line), and black markers show laboratory standards for carboxylic acids [from Alfarra, 2004].

0.19) to AMS  $m/z$  44 mass normalized by OM. The expected correlation of carboxylic acid groups with AMS  $m/z$  44 mass fraction (and thus with oxygenated organic aerosol, OOA) results from the efficient production of  $m/z$  44 mass fragments from monocarboxylic and dicarboxylic acids in the AMS [Alfarra, 2004], but  $m/z$  44 fragments may also be associated with nonacidic oxygenated groups. Both  $m/z$  44 mass fraction ( $r = 0.26$ ) and alcohol group mass fraction ( $r = 0.22$ ) had weak correlations to sulfate fraction, suggesting that sulfate fraction may be associated with alcohol and OOA components in Houston.

#### 4.2. Organic Composition of GAM, SAM, and NAM

[20] Organic mass (OM) and organic carbon (OC) mass are correlated to each other and to all organic functional groups that were present above detection limits. These correlations are partly a consequence of measuring organic molecules by their functional groups, since each carboxylic acid group is likely associated with one or more alkane groups. However, FTIR OM and functional groups also increase with AMS OM, OOA, and hydrocarbon-like organic aerosol (HOA) as well as WSOC, with varying degrees of correlation and scatter. These correlations reflect the fact that the main sources of organic compounds tend to covary to some degree, such that “polluted” NAM have more of all measured components, and “less polluted” GAM and SAM have less of all components. This result

is consistent with previous findings for FTIR and AMS measurements in Houston and other regions [Bates *et al.*, 2008; Gilardoni *et al.*, 2007; Kondo *et al.*, 2007]. Figure 2 identifies the GAM, SAM, and NAM (air masses identified by Bates *et al.* [2008] using radon concentration and back trajectories) and shows that the GAM types have the lowest OM concentration with  $2.0 \pm 1.0 \mu\text{g m}^{-3}$ , the SAM slightly more at  $3.5 \pm 1.8 \mu\text{g m}^{-3}$ , and the NAM the highest at  $8.6 \pm 4.5 \mu\text{g m}^{-3}$ .

[21] Characterizing the types of organic components on which OM properties depend requires consideration of the fraction of each component normalized to the appropriate total, where we have chosen to use the measured organic mass (for AMS and FTIR) or organic carbon mass (for WSOC) as the relevant total. The breakdown of normalized organic functional group fractions shown in Table 1 is generally similar among all three air mass types, which is not an unusual result for a localized, 1-month study. However, the normalized oxygenated organic group mass fractions showed that carboxylic acid groups in NAM (35%) were significantly higher than SAM (29%) and GAM (26%) at the 95% confidence level, as shown in Figure 5. Higher concentrations of alcohol groups were present in GAM (18% compared to 13% for NAM and SAM).

[22] Since negligible or very low concentrations of non-carboxylic carbonyl groups were measured, the sum of carboxylic acid groups (with O/C of 2) and alcohol groups (with O/C of 1) is normalized by the sum of all carbons present to give the O/C of the organic mass. The lower carboxylic acid fraction in the GAM is partially compensated by its higher alcohol fraction and likewise with the lower alcohol and higher acid groups in the NAM and SAM, so that the average O/C for all three air mass types is approximately 0.46, with the range extending from 0.40 for SAM to 0.51 for NAM. The AMS  $m/z$  44 mass fraction shows more variability, with the highest air mass sector average AMS  $m/z$  44 mass fraction of 0.16 in GAM and the lowest of 0.10 in SAM.

#### 4.3. Spectral Clusters for GAM, SAM, and NAM

[23] Ward cluster analysis was used to identify similarities among the measured organic spectra. Ward’s minimum variance method selects mutually exclusive hierarchical groups on the basis of the minimum error sum of squares, with the error being defined relative to the cluster center or mean [Ward, 1963]. The Ward cluster analysis resulted in two distinct classes of normalized FTIR spectra, which we named S and N and which each consisted of two subcategories (labeled S1, S2 and N1, N2). The spectra from these four clusters are shown in Figure 1. Figure 6 shows that the S1 and S2 clusters corresponds almost exactly to the spectra measured for particles in GAM and SAM, and the N1 and N2 clusters were found almost exclusively in particles measured in NAM. This categorization reflects both different kinds of organic compounds and different relative amounts of each organic functional group. The N1 and N2 cluster spectra have larger carboxylic acid group mass fractions, which are associated with a distinctive absorbance feature between 2600 and 2800 wave numbers. All of the N2 spectra are from NAM, but the N1 spectra include both

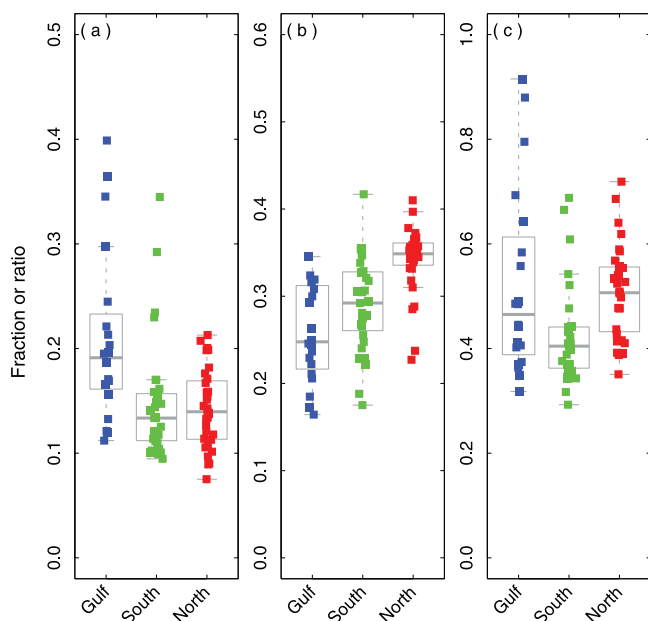


**Figure 5.** Comparison of mean and variability of (a) alcohol group, (b) carboxylic acid group, and (c) O/C fractions for GAM (blue), SAM (green), and NAM (red). Superposed bar indicates median value, box encompasses interquartile range, and whiskers extend to 1.5 times the interquartile range of the data.

spectra from NAM and SAM. S1 and S2 spectra are almost all from SAM and GAM.

#### 4.4. Organic Aerosol Factors for GAM, SAM, and NAM

[24] Positive matrix factorization (PMF) was applied to the FTIR spectra and XRF data using from 3 to 6 factors for the organic functional group range of 112 base-lined FTIR spectra (described in auxiliary material Text S1 and Table S1) collected for FTIR during TexAQS/GoMACCS [Paatero and Tapper, 1994], with details describing the implementation of the algorithm in auxiliary material Text S2. This set of number of factors was chosen on the basis of a singular value decomposition and fixed-size moving window analysis of the data matrix. The solution presented for each number of factors is approximately representative of the general class of solutions with varying degrees of rotation. While this short-term study does not provide sufficient statistical trends for detailed source apportionment, PMF and correlations with trace metals were used to estimate the contributions to organic functional groups of some generic source types. The results of PMF solutions dividing OM into 3, 4, 5, and 6 factors are shown in Figure 7, and their functional group composition is summarized in Table 2 for GAM, SAM, and NAM. None of the factor strengths identified by PMF has even a weak correlation ( $0.25 < r < 0.5$ ) with any of the functional group concentrations, showing that the time series are probably dominated by the sources of the organic components and that each of these sources is a mixture of multiple functional groups. Each of the time series of factor strengths was correlated with the time series of elemental concentrations measured by XRF.

For each factor, correlations to metals with  $r > 0.5$  or  $0.25 < r < 0.5$  are listed in Table 2.

[25] Three main source types were consistently identified with factors in the data set. Two of the factors were responsible for more than half the organic mass and were correlated with some typical combustion tracers (S, K, Se, Br, Pb) [Qureshi *et al.*, 2006; Sharma and Maloo, 2005] but had small differences in the degrees of correlation to other trace metals. The larger of the combustion factors was associated with the first combustion type, which was mildly or strongly correlated to additional elements often found for oil burning and refining processes (V, Cr, Ni, Zn, As) [Schroeder *et al.*, 1987; Finlayson-Pitts and Pitts, 2000; Qureshi *et al.*, 2006] as well as Sn. The OM in this factor is mostly alkane groups (52–57%) with carboxylic acid groups accounting for the next largest fraction (30–35%). The second combustion factor was mildly or strongly correlated to some similar fossil fuel trace metals (Cr, As) but the weaker signature for V and Ni suggests that wood smoke or coal burning are more likely to be the source of organic components in this factor rather than oil [Schroeder *et al.*, 1987; Finlayson-Pitts and Pitts, 2000; Qureshi *et al.*, 2006; Buzcu *et al.*, 2006; Buzcu-Guven and Fraser, 2008; Reimann *et al.*, 2008]. The identification of this factor with wood smoke is consistent with the strong correlation of its factor strength ( $r > 0.8$  for 3–6 factors) with m/z60, which is typically associated with levoglucosan (an organic marker for biomass burning) [Schneider *et al.*, 2006]. The composition of this wood smoke factor had the largest differences for different numbers of factors, but typically included a lower fraction of alkane groups than the first

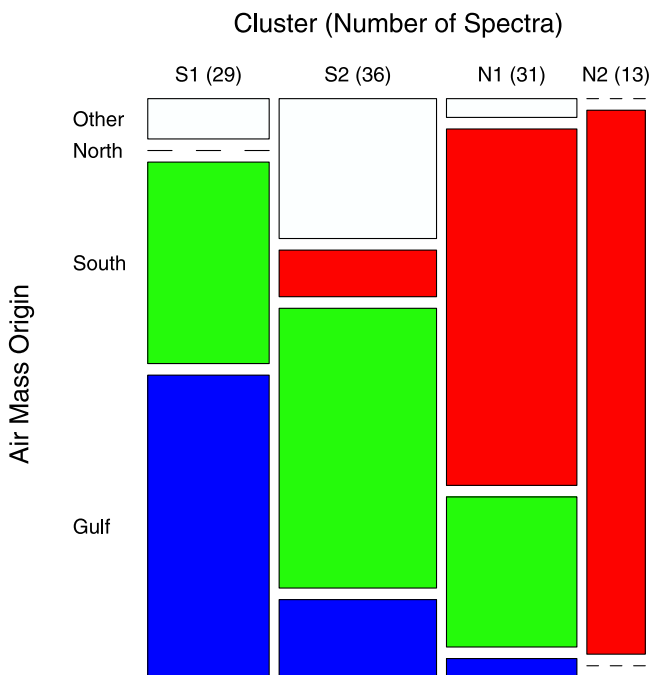


**Figure 6.** Cluster-sector comparison plot showing the number of samples associated with clusters S1, S2, N1, and N2 for each air mass sector. Colors indicate GAM (blue), SAM (green), and NAM (red).

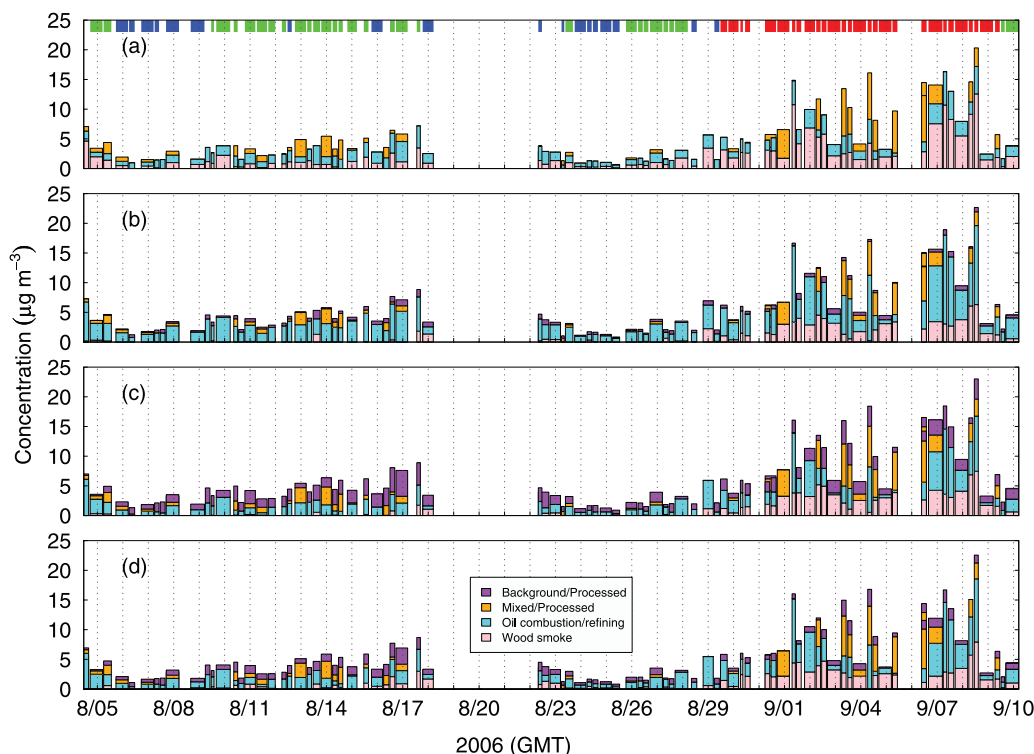


**Figure 7.** OM concentrations of oil combustion (teal), wood smoke (pink), secondary (orange), and background (purple) factors for (a) three-, (b) four-, (c) five-, and (d) six-factor PMF with GAM (blue), SAM (green), and NAM (red) marked by top colored bars.

(oil) factor (27–52%) and significant fractions of carboxylic acid groups (9–24%), nonacid carbonyl groups (12–32%), and amine groups (6–8%).

[26] The third factor that represented a significant fraction of OM mass in all PMF runs was only weakly correlated ( $0.25 < r < 0.5$ ) to some of the typical combustion elements (S, Br, Pb) [Schroeder *et al.*, 1987; Finlayson-Pitts and Pitts, 2000; Sharma and Maloo, 2005]. The weak correlation of this factor to source-specific conservative metal tracers indicates that it is likely more dependent on atmospheric processing than on the emissions of a single source type. The mix of associated metals to which there is a weak correlation is consistent with oil or coal combustion sources, although motor vehicle and industrial VOC sources in Houston, Dallas, and neighboring areas might have also contributed since no clear signature is evident. This “mixed” factor has more than one third (36–48%) carboxylic acid groups, which is consistent with atmospheric processing allowing for oxidation of organic compounds.

[27] For PMF with four or more factors, the fourth and fifth factors were only weakly correlated to S and four combustion metals (Sn, V, Ni, Pb). The fourth factor is likely to be from distant and diluted natural or man-made sources as it appears in similarly small amounts ( $0.3\text{--}1.5\ \mu\text{g m}^{-3}$ ) for all three types of air masses (GAM, SAM, and NAM). The low, nonsector-dependent concentration provides some evidence that this particle factor may be associated with a “background” organic component with equal contributions in Gulf and continental regions, possibly associated with remote sources that produce organic components with long enough lifetimes to be globally dispersed. The fifth factor

represents a small fraction of OM, and is associated with elemental signatures typical of dust ( $r > 0.5$  for Al, Si, Ca;  $0.25 < r < 0.5$  for K, Ti, Fe) [Li *et al.*, 2004; Balasubramanian and Qian, 2004]. While there is significant ancillary evidence of Saharan dust particles, the number of samples was insufficient to clearly identify dust as the source of the OM in this factor. The sixth factor in the 6 factor simulation was sampled too infrequently to identify and accounted for less than  $0.1\ \mu\text{g m}^{-3}$  for GAM and SAM and only  $0.6\ \mu\text{g m}^{-3}$  of NAM.

## 5. Discussion

[28] The organic functional groups measured in the Houston area show how the organic mass and oxygenated fraction of organic mass vary with different air mass sectors and source types. In addition, we can evaluate how these components are affected by diurnal trends, volatility, and aging. Finally we consider how the organic components affect the CCN activity, aerosol optical hygroscopic growth factor ( $f(\text{RH})$ ), and WSOC.

### 5.1. Sources of Oxygenated Organic Compounds

[29] The NAM have a significantly higher fraction of carboxylic acid than either the GAM or SAM, and this difference is highlighted by the strong distinction in normalized spectral shape between cluster categories N1 and N2 compared to S1 and S2. On the other hand, the GAM have significantly higher alcohol groups than both the SAM and NAM. The combined effect is that the O/C is very similar

Table 2. Average Organic Mass and Major Functional Group Mass Contributions of PMF Factors by Air Mass Origin

	Three Factors			Four Factors			Five Factors			Six Factors		
	Average Organic Mass ( $\mu\text{g m}^{-3}$ )			Average Organic Mass ( $\mu\text{g m}^{-3}$ )			Average Organic Mass ( $\mu\text{g m}^{-3}$ )			Average Organic Mass ( $\mu\text{g m}^{-3}$ )		
	GAM	SAM	NAM									
Oil combustion/refining ( $r > 0.5$ : S, K, Se, Br, Pb, V, Cr, Ni, Zn, As, Rb, In, Sn, La)	1.1	1.2	1.8	1.5	2.4	3.2	0.8	1.6	2.1	0.9	1.5	2.4
Alkane groups			52%			57%			57%			56%
Carboxylic acid groups			30%			30%			35%			35%
Alcohol groups			11%			10%			5%			5%
Amine groups			5%			3%			4%			4%
O/C			0.38			0.35			0.35			0.35
Wood smoke ( $r > 0.5$ : S, K, Se, Br, Pb, Cr, As, La)	0.5	1.0	3.3	0.2	0.2	2.8	0.1	0.2	3.0	0.3	0.4	2.8
Alkane groups			52%			50%			30%			27%
Carboxylic acid groups			24%			9%			22%			20%
Nonacid carbonyl groups			12%			32%			29%			31%
Amine groups			8%			8%			8%			6%
O/C			0.34			0.31			0.61			0.65
Mixed/Processed ( $0.25 < r < 0.5$ : S, Br, Ag, Pb)	0.2	0.5	1.5	0.2	0.4	1.1	0.2	0.4	1.4	0.2	0.4	1.3
Alkane groups			43%			37%			39%			52%
Carboxylic acid groups			44%			48%			47%			36%
O/C			0.57			0.69			0.66			0.44
Background ( $0.25 < r < 0.5$ : S, V, Ni, Sn, Zn)	-	-	-	0.3	0.3	0.6	1.1	1.1	1.5	0.7	0.8	0.7
Alkane groups			-			33%			54%			57%
Alcohol groups			-			41%			21%			26%
O/C			-			0.61			0.37			0.33
Soil dust ( $r > 0.5$ : Al, Si, Ca, Sr; $0.25 < r < 0.5$ : K, Ti, Fe, Y)	-	-	-	-	-	-	0.2	0.2	0.4	0.2	0.2	0.4
Unidentified ( $0.25 < r < 0.5$ : S, V, Ni, Sn, Sb)	-	-	-	-	-	-	-	-	-	0.0	0.1	0.6

for the NAM and GAM despite their different composition, and SAM have a slightly lower mean O/C.

[30] PMF factors attribute alkane, carboxylic acid, and alcohol groups largely to metal-producing emissions sources, which were dominated by oil combustion for all air masses. For GAM, the oil combustion was probably dominated by shipping activities, as was suggested previously on the basis of the high sulfur concentrations and the large amount of shipping activity in the Gulf of Mexico [Bates *et al.*, 2008]. For SAM and NAM, oil-combustion activities (including shipping and petrochemical operations) in and near the port were still an important source, but wood smoke also contributed to OM (and to carboxylic acid and amine groups). Many of the petrochemical operations and power plants in the Houston metropolitan area are oil- or gas-fired [Buzcu-Guyen and Fraser, 2008], but agricultural wood burning in East Texas has been shown to be an important source of OM in Houston during August and September. The Parish Power Plant southwest of Houston and several power plants in the Dallas area are partially or completely fired by coal or lignite [Brock *et al.*, 2003] (<http://www.epa.gov/cleanenergy/energy-resources/egrid/index.html>), which could also contribute to the wood smoke factor since the trace metal signatures for coal and wood burning can be similar. The alcohol groups are likely associated with wood smoke, with measurements in Mexico City linking alcohol group concentrations to biomass burning [Liu *et al.*, 2009]. The “processed” factor with the highest fraction of acid groups is 2 or 3 times larger in the NAM than the GAM or SAM, and this third factor probably accounts for its high acid fraction. This factor is likely to be dominated by secondary sources, since it has only weak correlations to trace elements. Given the northerly origin of these air masses, emissions from Dallas or other areas in East Texas that are multiple days upwind could have undergone processing in the atmosphere to produce the high fraction of carboxylic acid groups (36–48%).

[31] In the NAM, 5.1–6.0  $\mu\text{g m}^{-3}$  of the 8.6  $\mu\text{g m}^{-3}$  of OM is associated with wood or oil combustion factors, and 1.1–1.5  $\mu\text{g m}^{-3}$  with OM formed from processed organic aerosol. An additional 0.6–1.5  $\mu\text{g m}^{-3}$  is associated with background, dust or other unidentified OM sources. Thus, the organic concentrations and composition indicate that atmospheric processing accounts for about one fourth of the OM measured in NAM. More than a third (36–48%) of this processed OM is carboxylic acid groups, resulting in a substantial increase in the acid fraction associated with the NAM.

[32] Most of the O/C in the measured ambient aerosol is attributed by PMF to the oil and wood combustion emissions. For example, the four-factor PMF identification of NAM attributes 3.2  $\mu\text{g m}^{-3}$  to oil combustion emissions with O/C of 0.34 and 2.8  $\mu\text{g m}^{-3}$  to wood smoke emissions with O/C of 0.31, which together account for almost two thirds of the total 8.6  $\mu\text{g m}^{-3}$  average concentration and O/C of 0.51. This result indicates that the O/C from NAM is largely the result of emissions from combustion sources rather than processing, in other words most of the oxygenated organic groups came from nonprocessed emissions. Similar relationships exist for the GAM and SAM, suggesting that combustion sources dominate the production of oxygenated organic compounds in this region.

[33] Bates *et al.* [2008] noted the significant contributions of soil dust to the mass of submicron particles in the GAM and SAM. However, very little OM was associated with the measured trace metals that are typical of dust emissions. Nonetheless, it is possible that OM derived from other sources or formed through atmospheric processing condensed onto the dust particles yielding an internal mixture.

## 5.2. Diurnal Trends and Aging

[34] There is no evidence for a noontime or afternoon maximum in O/C from either time-resolved AMS or the multihour FTIR filters, which suggests that the organic oxidation that occurred was either very fast (i.e., instantaneously after emission) or was slower than the 6- to 12-h time scale on which photochemically produced oxidants change concentration rapidly [Maria *et al.*, 2004]. Rapid production of OM and increases in O/C are consistent with the large fraction of the oxidized organic groups associated with metal tracers of combustion emissions. Thus the similarity of daytime and nighttime organic composition may indicate that the oxidation processes in this particularly polluted region are not photochemically limited.

[35] The addition of SOA to the particle phase (resulting in increased OM) is sometimes referred to as “aging” but frequently this term refers more specifically to oxidation of gas or particle-phase organics by atmospheric oxidants to form organic compounds with higher O/C. This higher O/C is interpreted as the addition of carboxylic acid groups (with O/C up to 2) and alcohol groups (with O/C up to 1) to the initially emitted hydrocarbons (with O/C of 0). In this work we consider separately increases in OM from secondary sources and increases in O/C from atmospheric oxidation (in both gas and particle phases). The assumption that OM or O/C increases occur during hours to days of atmospheric processing rather than at or soon after emission is implicit in the term “aging,” which requires that the time since emission (for “emitted” OM) or the time available for atmospheric processing (for “processed” OM) be known. The Houston area was affected by multiple sources from all directions, making Lagrangian or tracer-derived aging time estimates inapplicable. The mild to strong correlation of the OM from the two combustion factors to the trace metals suggests that this OM and associated O/C formed relatively quickly (perhaps a few hours), as longer time lags would have resulted in poorer correlations. The measured O/C for both the “emitted” combustion-derived factors and the “processed” factor were very similar, which does not support the idea that more processed organics would be aged in the sense of having higher O/C. The processed factor did include a larger fraction of oxygen from carboxylic acid groups rather than alcohols, in keeping with the formation of carboxylic acid groups during extended atmospheric processing or “aging.”

[36] It is worth noting that the “emitted” carboxylic acid group concentration is likely to include both primary and secondary sources, as VOCs coemitted with the metals may condense quickly enough to be correlated in time with the metals in the primary particles. The distinction of “emitted” versus “processed” does not distinguish between primary and secondary per se. Rather it addresses the regulatory interest of whether the OM came from combustion or some other VOC or POA source. The term “emitted” refers to

OA from a particular identified source (whether it was emitted as VOC or POA), and the term “processed” indicates SOA which involved emissions from more than one source (e.g., biogenic VOCs and vehicle-derived oxidants) or which required sufficient processing time that they lost their correlation in time to the primary metals from the same source.

### 5.3. Organic Volatility

[37] Primary particles form at or very near their point of emission from the source into the atmosphere. Secondary particles form in the atmosphere, entirely from components emitted in the gas phase. The distinction between primary and secondary aerosol particles then relies on whether a particular component was in the gas or particle phase at emission, with the temperature at emission typically changing rapidly and being poorly quantified. Hence, the definition of primary particles depends on the timescale and temperature at which the particle phase is “emitted,” making this identification very ambiguous for many ambient and laboratory aerosol systems [Robinson *et al.*, 2007].

[38] Simultaneous short (<14 h) and long (~24 h) samples were collected for quality control and assurance. The long samples had increased time for evaporation or desorption of semivolatile organic compounds during collection. It is likely that the organic components that decreased during the longer samples were more volatile than the rest of the OM. The comparison of composition of the short and long samples in the inset of Figure 2 indicates that the long samples had lost one third to one half of the alkane and carboxylic acid group mass during the extended sampling, although the changes in alcohol group mass were very small. The loss of OM indicates a semivolatile aerosol that would lead to different amounts of primary particles depending on emission temperature.

### 5.4. Water Uptake by Organic Components From CCN, WSOC, and f(RH)

[39] Atmospheric observations in a variety of regions have provided evidence that organic components can play important roles in water uptake in subsaturated and supersaturated conditions, including as CCN for cloud droplets [Liu *et al.*, 1996; Russell *et al.*, 2000; Kaku *et al.*, 2006; Twohy *et al.*, 2005; Maria and Russell, 2005; Hawkins *et al.*, 2008]. For the Houston region, Quinn *et al.* [2007] have discussed the role of HOA in increasing the minimum diameter of cloud nucleating particles as reflected in the measured increases in the critical diameter required for activation at 0.44% supersaturation as the HOA mass fraction increased. This anticorrelation with critical diameter also is evident in submicron HOA/POM. This finding is consistent with the tracking of HOA below 200 nm with submicron HOA [Bates *et al.*, 2008]. The corollary is also supported, namely that a higher fraction of OOA increases the number of CCN at 0.44% supersaturation. CCN/CN (CCN normalized by total condensation nuclei) is correlated strongly with OOA/OM with  $r = 0.81$ . (The complementary anticorrelation of HOA/POM with CCN/CN has  $r = -0.65$ .) In keeping with the relationship of OOA/POM to CCN/CN, the oxygenated organic fraction is correlated with CCN/CN for both AMS  $m/z$  44 mass fraction ( $r = 0.79$ ) and FTIR O/C ( $r = 0.59$ ).

[40] The observed correlations of alcohol and amine groups to CCN are weak ( $r = 0.47$  for alcohol group fraction and  $r = 0.35$  for amine group fraction), and there is even less of a correlation of carboxylic acid group fraction to CCN/CN ( $r = 0.18$ ). The strongest relationship between organic functional group fractions and CCN/CN is found in the anticorrelation of alkane group mass fraction to CCN/CN ( $r = -0.65$ ) which effectively mirrors the mild correlation of FTIR O/C since alkane groups dominate the denominator. While multiple functional groups correlate with increased CCN activity, the absence of nonaliphatic groups reflected in the high alkane group fraction is perhaps the best single predictor of lower CCN fraction.

[41] Kondo *et al.* [2007] and Bates *et al.* [2008] reported a correlation between WSOC and OOA; however, WSOC normalized by submicron OC (by offline analysis with a Sunset EGA [Bates *et al.*, 2008]) correlates positively but weakly with carboxylic acid group mass fraction ( $r = 0.40$ ) and negatively but more weakly with both alcohol group mass fraction ( $r = -0.37$ ) and AMS OOA fraction ( $r = -0.22$ ). An underlying correlation between WSOC and acid fractions may be partially masked by other components [Kaku *et al.*, 2006; Miyazaki *et al.*, 2007]. The weak correlation of WSOC/OC with the nitrate fraction of PM1 ( $r = 0.35$ ) contrasts with its weak anticorrelations to sulfate mass fraction of PM1 ( $r = -0.30$ ). Figure 8 shows that WSOC/OC does not correlate with CCN/CN, which is consistent with the nonexistent or weak correlations of WSOC/OC and OOA/OM, O/C, and carboxylic acid mass fraction.

[42] Sulfate fraction had a weak correlation to CCN/CN ( $r = 0.31$ ) but a mild correlation to  $f(\text{RH})$  at  $r = 0.66$ . Nitrate and organic fractions of PM were weakly anticorrelated to  $f(\text{RH})$  ( $r = -0.40$  and  $-0.36$ , respectively). The anticorrelation of the organic fraction is weaker than reported by Massoli *et al.* [2009], both because it is normalized by PM rather than OM plus sulfate and because it includes the entire TexAQS/GoMACCS sampling period. Carboxylic acid group mass fraction was also weakly anticorrelated to  $f(\text{RH})$  with  $r = -0.41$ , consistent with earlier findings [Quinn *et al.*, 2007].

[43] Summarizing only the correlations that exceed  $r = 0.5$  for the Houston region sampled here, CCN is associated most strongly with the organic O/C or oxidized organic fraction, whereas  $f(\text{RH})$  is correlated strongly only with the sulfate fraction ( $r = 0.66$ ). Neither of these relationships or any correlation with  $r > 0.5$  was found with WSOC/OC for TexAQS/GoMACCS. The absence of a correlation of O/C (or alcohol fraction) with WSOC/OC could result from a lack of collection, solubility, or transmission of the alcohol or phenol components of the oxygenated organic fraction in the condensed aqueous solution of the PLS instrument. Similarly, the observed distinction between the chemical components that influence CCN and  $f(\text{RH})$  is expected given the differences in sampling bias (CCN is dominated by submicron number distribution, but  $f(\text{RH})$  is controlled by submicron mass distribution), which are inherent to comparing ambient measurements by CCN counters and nephelometers. However, this result is also consistent with organic particles influencing CCN by a property other than hygroscopicity, since the oxygenated organics seem to have little role in the hygroscopicity measured by  $f(\text{RH})$ . This

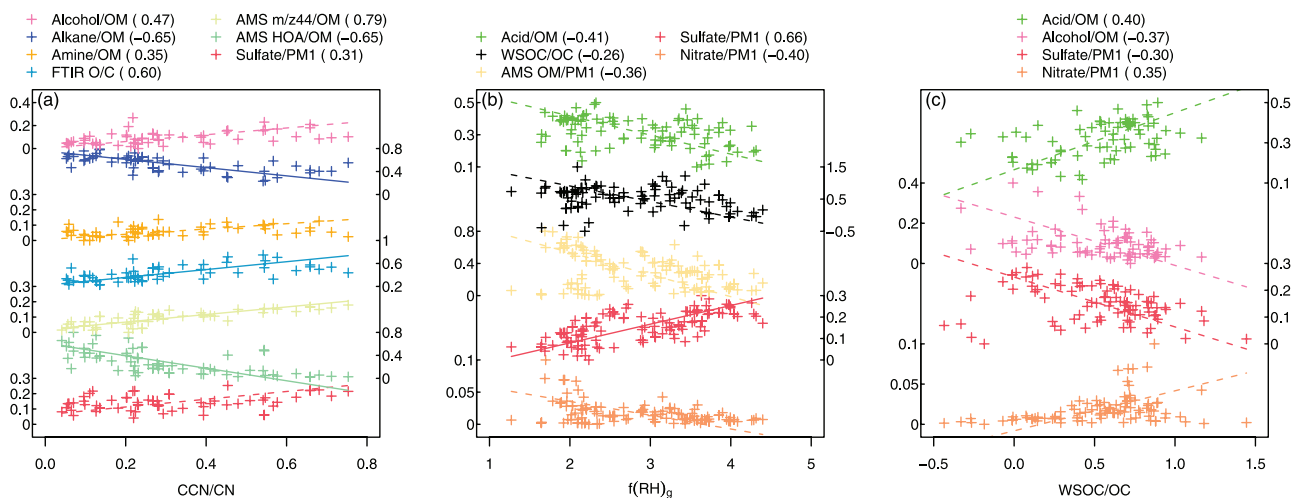


**Figure 8.** Scatterplots showing correlations between (a) CCN/CN, (b)  $f(\text{RH})$  from blue, green, and red wavelength scattering, and (c) WSOC/OC to normalized FTIR functional groups and O/C, normalized AMS HOA and O/C, and sulfate and nitrate mass normalized to total submicron mass (PM1). The Pearson's  $r$  coefficients are given in the legend; solid lines are shown for mild and strong correlations ( $|r| > 0.5$ ) and dotted lines for weak correlations ( $0.25 < |r| < 0.5$ ) simply to serve as a guide for the eye. Measurements and line fits are omitted for all components with  $|r| < 0.25$ .

property could be surface tension or mass accommodation coefficient, since both of these characteristics are more likely to affect CCN than  $f(\text{RH})$  measurements.

## 6. Conclusions

[44] Organic mass concentrations derived from FTIR functional group analysis on filter samples showed good agreement with AMS concentrations averaged over the filter collection periods ( $r = 0.84$ ). The ambient concentrations ranged from 1 to  $25 \mu\text{g m}^{-3}$  and varied significantly with the wind direction associated with the sampled air masses. NAM had passed over land for several days before being sampled. These air masses were influenced by continental sources during transport and had longer times since emission for atmospheric processing to occur than SAM. Averaged over the entire experiment, the organic mass consisted mostly of alkane groups (47%), with the fraction of organic mass identified as carboxylic acid groups accounting for 31% of OM. Significantly higher carboxylic acid group mass fractions were found for NAM (25%) than SAM (29%) or GAM (29%). The carboxylic acid group fractions in the GAM and SAM included ship emissions as well as background marine sources but little (SAM) or no (GAM) recent land influences (based on radon concentrations).

[45] PMF analysis was used to identify four main factors in the measured organic functional groups: emitted from oil combustion or refining, emitted from wood smoke, processed from mixed sources, and background sources. While the composition and fractional contribution varied somewhat with the specifications used in the factorization, several trends in composition were robust for the entire range of factors and rotations selected. Carboxylic acid group mass fractions of 30–35% were associated with factors that had mild or strong correlations ( $r > 0.5$ ) with elements typical of oil combustion, indicating that the acid fraction formed was

largely independent of atmospheric conditions or processing (even if it occurred after emission). Higher carboxylic acid group mass fractions (36–48%) were associated with factors that were poorly correlated with trace metals ( $r < 0.5$ ), suggesting that the higher than average carboxylic acid group fractions (and the associated higher O/C) were associated with atmospheric oxidation processes that occurred downwind over longer time scales. Alcohol groups were also associated with combustion emissions and background sources, accounting for 5–11% of oil combustion factor OM and 12–46% of background OM factor. Amine groups accounted for approximately 4% of GAM, SAM, and NAM, with high concentrations (6–8%) associated with the wood smoke factor.

[46] Since it is not possible to distinguish between primary and secondary particles during ambient sampling, here we have distinguished between organic particle components associated directly with emissions from a single source type, which track proportionally to coemitted nonvolatile metals, and those which are “processed” in the atmosphere, for which time since emission, light, oxidant concentrations, relative humidity, and meteorology may control their formation. Mild and strong correlations to nonvolatile trace metal signatures are used to identify organic mass associated with primary particle sources, and weak correlations with coemitted combustion metals are used to identify organic mass for which atmospheric processes account for some of the variability in OM produced. The organic concentrations and composition indicate that atmospheric processing accounts for about one fourth of the OM measured in NAM. More than a third (36–48%) of this processed OM is carboxylic acid groups, resulting in a substantial increase in the acid fraction associated with the NAM. All of the PMF results suggest that while the processed aerosol has the highest O/C (e.g., 0.65), most of the O/C in the measured ambient aerosol is directly associated with the oil and wood

combustion emissions. This result indicates that the O/C from NAM is largely the result of emissions of oxidizable components from a defined set of sources rather than processing. This finding also holds for the GAM and SAM, in which wood smoke emissions have negligible contributions to the O/C but the oil-combustion emissions still contribute significant fractions of carboxylic acid groups to the OM and O/C.

[47] Alcohol (including phenol) and amine group mass fractions showed weak correlations ( $r = 0.47$  and  $0.35$ ) with CCN/CN, and alkane mass fraction showed a mild anti-correlation ( $r = -0.65$ ). FTIR O/C and AMS  $m/z$  44 mass fraction showed mild ( $r = 0.60$ ) and strong ( $0.79$ ) correlations, respectively, to CCN/CN. Sulfate fraction had a weak correlation with CCN/CN and mild correlation to  $f(\text{RH})$ .

[48] **Acknowledgments.** Sample collection and preliminary analysis were supported by the National Oceanic and Atmospheric Administration NA17RJ1231; method development and statistical analysis to quantify anthropogenic organic components were supported by an award from the James S. McDonnell Foundation. We thank Stefania Gilardoni, Derek Coffman, Drew Hamilton, Catherine Hoyle, and the crew of the NOAA R/V *Ronald Brown* for assistance in preparing and collecting filters for FTIR and XRF analysis. We also acknowledge helpful comments from Matt Fraser, Pentti Paatero, Greg Frost, Jose Jimenez, and Doug Worsnop.

## References

- Aiken, A. C., et al. (2008), O/C and OM/OC ratios of primary, secondary, and ambient organic aerosols with high resolution time-of-flight aerosol mass spectrometry, *Environ. Sci. Technol.*, *42*, 4478–4485, doi:10.1021/es703009q.
- Alfarra, M. R. (2004), Insights into atmospheric organic aerosols using an aerosol mass spectrometer, Ph.D. thesis, Univ. of Manchester, Manchester, U.K.
- Allan, J. D., J. L. Jimenez, P. I. Williams, M. R. Alfarra, K. N. Bower, J. T. Jayne, H. Coe, and D. R. Worsnop (2003), Quantitative sampling using an Aerodyne aerosol mass spectrometer: 1. Techniques of data interpretation and error analysis, *J. Geophys. Res.*, *108*(D3), 4090, doi:10.1029/2002JD002358.
- Balasubramanian, R., and W. B. Qian (2004), Characterization and source identification of airborne trace metals in Singapore, *J. Environ. Monit.*, *6*, 813–818, doi:10.1039/b407523d.
- Bates, T. S., et al. (2008), Boundary layer aerosol chemistry during TexAQS/GoMACCS 2006: Insights into aerosol sources and transformation processes, *J. Geophys. Res.*, *113*, D00F01, doi:10.1029/2008JD010023.
- Brock, C. A., et al. (2003), Particle growth in urban and industrial plumes in Texas, *J. Geophys. Res.*, *108*(D3), 4111, doi:10.1029/2002JD002746.
- Buzcu, B., Z. W. Yue, M. P. Fraser, U. Nopmongkol, and D. T. Allen (2006), Secondary particle formation and evidence of heterogeneous chemistry during a wood smoke episode in Texas, *J. Geophys. Res.*, *111*, D10S13, doi:10.1029/2005JD006143.
- Buzcu-Guven, B., and M. P. Fraser (2008), Comparison of VOC emissions inventory data with source apportionment results for Houston, TX, *Atmos. Environ.*, *42*, 5032–5043, doi:10.1016/j.atmosenv.2008.02.025.
- Carrico, C. M., M. J. Rood, J. A. Ogren, C. Neusuess, A. Wiedensohler, and J. Heintzenberg (2000), Aerosol optical properties at Sagres, Portugal during ACE-2, *Tellus, Ser. B*, *52*, 694–715.
- Decesari, S., M. Mircea, F. Cavalli, S. Fuzzi, F. Moretti, E. Tagliavini, and M. C. Facchini (2007), Source attribution of water-soluble organic aerosol by nuclear magnetic resonance spectroscopy, *Environ. Sci. Technol.*, *41*, 2479–2484, doi:10.1021/es061711i S0013–936X(06)01711–1.
- Ervens, B. G. Feingold, and S. M. Kreidenweis (2005), Influence of water-soluble organic carbon on cloud drop number concentration, *J. Geophys. Res.*, *110*, D18211, doi:10.1029/2004JD005634.
- Finlayson-Pitts, B. J., and J. N. Pitts (2000), Particles in the troposphere, in *Chemistry of the Upper and Lower Atmosphere*, pp. 386–388, Academic Press, San Diego, Calif.
- Gilardoni, S., et al. (2007), Regional variation of organic functional groups in aerosol particles on four U.S. east coast platforms during the International Consortium for Atmospheric Research on Transport and Transformation 2004 campaign, *J. Geophys. Res.*, *112*, D10S27, doi:10.1029/2006JD007737.
- Hawkins, L. N., L. M. Russell, C. H. Twohy, and J. R. Anderson (2008), Uniform particle-droplet partitioning of 18 organic and elemental components in DYCOMS-II stratocumulus clouds, *J. Geophys. Res.*, *113*, D14201, doi:10.1029/2007JD009150.
- Jayne, J. T., D. C. Leard, X. Zhang, P. Davidovits, K. A. Smith, C. E. Kolb, and D. R. Worsnop (2000), Development of an aerosol mass spectrometer for size and composition, *Aerosol Sci. Technol.*, *33*, 49–70, doi:10.1080/027868200410840.
- Jimenez, J. L., et al. (2003), Ambient aerosol sampling with an Aerodyne Aerosol Mass Spectrometer, *J. Geophys. Res.*, *108*(D7), 8425, doi:10.1029/2001JD001213.
- Kaku, K. C., D. A. Hegg, D. S. Covert, J. L. Santarpia, H. Jonsson, G. Buzorius, and D. R. Collins (2006), Organics in the northeastern Pacific and their impacts on aerosol hygroscopicity in the subsaturated and supersaturated regimes, *Atmos. Chem. Phys.*, *6*, 4101–4115.
- Kanakidou, M., et al. (2005), Organic aerosol and global climate modelling: A review, *Atmos. Chem. Phys.*, *5*, 1053–1123.
- Keller, H. R., and D. L. Massart (1992), Evolving factor analysis, Chemometr, *Intell. Lab. Syst.*, *12*, 209–224, doi:10.1016/0169-7439(92)80002-L.
- Kondo, Y., Y. Miyazaki, N. Takegawa, T. Miyakawa, R. J. Weber, J. L. Jimenez, Q. Zhang, and D. R. Worsnop (2007), Oxygenated and water-soluble organic aerosols in Tokyo, *J. Geophys. Res.*, *112*, D01203, doi:10.1029/2006JD007056.
- Li, Z., P. K. Hopke, L. Husain, S. Qureshi, V. A. Dutkiewicz, J. J. Schwab, F. Drewnick, and K. L. Demerjian (2004), Sources of fine particle composition in New York city, *Atmos. Environ.*, *38*, 6521–6529, doi:10.1016/j.atmosenv.2004.08.040.
- Liu, P. S. K., W. R. Leaitch, C. M. Banic, S.-M. Li, D. Ngo, and W. J. Megaw (1996), Aerosol observations at Chebogue Point during the 1993 North Atlantic Regional Experiment: Relationships among cloud condensation nuclei, size distribution and chemistry, *J. Geophys. Res.*, *101*(D22), 28,971–28,990.
- Liu, S., S. Takahama, L. M. Russell, S. Gilardoni, and D. Baumgardner (2009), Oxygenated organic functional groups and their sources in single and submicron organic particles in MILAGRO 2006 campaign, *Atmos. Chem. Phys. Discuss.*, *9*, 1–40. (Available at <http://aerosol.ucsd.edu/publications.html>)
- Liu, X., Y. Cheng, Y. Zhang, J. Jung, N. Sugimoto, S. Y. Chang, Y. J. Kim, S. Fan, and L. Zeng (2008), Influences of relative humidity and particle chemical composition on aerosol scattering properties during the 2006 PRD campaign, *Atmos. Environ.*, *42*, 1525–1536, doi:10.1016/j.atmosenv.2007.10.077.
- Mader, B. T., and J. F. Pankow (2001), Gas/solid partitioning of semivolatile organic compounds (SOCs) to air filters. 3. An analysis of gas adsorption artifacts in measurements of atmospheric SOC and organic carbon (OC) when using Teflon membrane filters and quartz fiber filters, *Environ. Sci. Technol.*, *35*, 3422–3432, doi:10.1021/es0015951.
- Maria, S. F., and L. M. Russell (2005), Organic and inorganic aerosol below-cloud scavenging by suburban New Jersey precipitation, *Environ. Sci. Technol.*, *39*, 4793–4800, doi:10.1021/es0491679.
- Maria, S. F., L. M. Russell, B. J. Turpin, and R. J. Porcja (2002), FTIR measurements of functional groups and organic mass in aerosol samples over the Caribbean, *Atmos. Environ.*, *36*, 5185–5196, doi:10.1016/S1352-2310(02)00654-4.
- Maria, S. F., L. M. Russell, B. J. Turpin, R. J. Porcja, T. L. Campos, R. J. Weber, and B. J. Huebert (2003), Source signatures of carbon monoxide and organic functional groups in Asian Pacific Regional Aerosol Characterization Experiment (ACE-Asia) submicron aerosol types, *J. Geophys. Res.*, *108*(D23), 8637, doi:10.1029/2003JD003703.
- Maria, S. F., L. M. Russell, M. K. Gilles, and S. C. B. Myneni (2004), Organic aerosol growth mechanisms and their climate forcing implications, *Science*, *306*, 1921–1925, doi:10.1126/science.1103491.
- Massoli, P., T. S. Bates, P. K. Quinn, D. A. Lack, T. Baynard, B. M. Lerner, S. C. Tucker, J. Brioude, A. Stohl, and E. J. Williams (2009), Aerosol optical and hygroscopic properties during TexAQS-GoMACCS 2006 and their impact on aerosol direct radiative forcing, *J. Geophys. Res.*, doi:10.1029/2008JD011604, in press.
- McMurry, P. H., M. Shepherd, and J. Vickery (Eds.) (2003), *Particulate Matter Science for Policy Makers: A NARSTO Assessment*, NARSTO, Pasco, Wash.
- Ming, Y., and L. M. Russell (2001), Predicted hygroscopic growth of sea salt aerosol, *J. Geophys. Res.*, *106*(D22), 28,259–28,274.
- Miyazaki, Y., Y. Kondo, S. Han, M. Koike, D. Kodama, Y. Komazaki, H. Tanimoto, and H. Matsueda (2007), Chemical characteristics of water-soluble organic carbon in the Asian Outflow, *J. Geophys. Res.*, *112*, D22S30, doi:10.1029/2007JD009116.
- Orsini, D. A., Y. L. Ma, A. Sullivan, B. Sierau, K. Baumann, and R. J. Weber (2003), Refinements to the particle-into-liquid sampler (PILS) for ground and airborne measurements of water soluble aerosol composition, *Atmos. Environ.*, *37*, 1243–1259, doi:10.1016/S1352-2310(02)01015-4.

- Paatero, P., and U. Tapper (1994), Positive matrix factorization: A non-negative factor model with optimal utilization of error estimates of data values, *Environmetrics*, *5*, 111–126, doi:10.1002/env.3170050203.
- Quinn, P. K., et al. (2006), Impacts of sources and aging on submicrometer aerosol properties in the marine boundary layer across the Gulf of Maine, *J. Geophys. Res.*, *111*, D23S36, doi:10.1029/2006JD007582.
- Quinn, P. K., T. S. Bates, D. J. Coffman, and D. S. Covert (2007), Influence of particle size and chemistry on the cloud nucleating properties of aerosols, *Atmos. Chem. Phys.*, *8*, 14,171–14,208.
- Qureshi, S., V. A. Dutkiewicz, A. R. Khan, K. Swami, K. X. Yang, L. Husain, J. J. Schwab, and K. L. Demerjian (2006), Elemental composition of PM<sub>2.5</sub> aerosols in Queens, New York: Solubility and temporal trends, *Atmos. Environ.*, *40*, Suppl. 2, 238–251, doi:10.1016/j.atmosenv.2005.12.070.
- Reimann, C., R. T. Ottesen, M. Andersson, A. Arnoldussen, F. Koller, and P. Englmaier (2008), Element levels in birch and spruce wood ashes—Green energy?, *Sci. Total Environ.*, *393*, 191–197, doi:10.1016/j.scitotenv.2008.01.015.
- Robinson, A. L., N. M. Donahue, M. K. Shrivastava, E. A. Weitkamp, A. M. Sage, A. P. Grieshop, T. E. Lane, J. R. Pierce, and S. N. Pandis (2007), Rethinking organic aerosols: Semivolatile emissions and photochemical aging, *Science*, *315*, 1259–1262, doi:10.1126/science.1133061.
- Russell, L. M. (2003), Aerosol organic-mass-to-organic-carbon ratio measurements, *Environ. Sci. Technol.*, *37*, 2982–2987.
- Russell, L. M., K. J. Noone, R. J. Ferek, R. A. Pockalny, R. C. Flagan, and J. H. Seinfeld (2000), Combustion organic aerosol as cloud condensation nuclei in ship tracks, *J. Atmos. Sci.*, *57*, 2591–2606, doi:10.1175/1520-0469(2000)057<2591:COAACC>2.0.CO;2.
- Schneider, J., S. Weimer, F. Drewnick, S. Borrmann, G. Helas, P. Gwaze, O. Schmid, M. O. Andreae, and U. Kirchner (2006), Mass spectrometric analysis and aerodynamic properties of various types of combustion-related aerosol particles, *Int. J. Mass Spectrom.*, *258*, 37–49, doi:10.1016/j.ijms.2006.07.008.
- Schroeder, W. H., M. Dobson, D. M. Kane, and N. D. Johnson (1987), Toxic trace elements associated with airborne particulate matter: A review, *J. Air Pollut. Control Assoc.*, *37*, 1267–1285.
- Sharma, M., and S. Maloo (2005), Assessment of ambient air PM<sub>10</sub> and PM<sub>2.5</sub> and characterization of PM<sub>10</sub> in the city of Kanpur, India, *Atmos. Environ.*, *39*, 6015–6026, doi:10.1016/j.atmosenv.2005.04.041.
- Shilling, J. E., S. M. King, M. Mochida, D. R. Worsnop, and S. T. Martin (2007), Mass spectral evidence that small changes in composition caused by oxidative aging processes alter aerosol CCN properties, *J. Phys. Chem. A*, *111*(17), 3358–3368, doi:10.1021/jp068822r.
- Shilling, J. E., et al. (2008), Loading-dependent elemental composition of  $\alpha$ -pinene SOA particles, *Atmos. Chem. Phys. Discuss.*, *8*, 15,343–15,373.
- Simoneit, B. R. T., M. Kobayashi, M. Mochida, K. Kawamura, M. Lee, H. J. Lim, B. J. Turpin, and Y. Komazaki (2004), Composition and major sources of organic compounds of aerosol particulate matter sampled during the ACE-Asia campaign, *J. Geophys. Res.*, *109*, D19S10, doi:10.1029/2004JD004598.
- Sorooshian, A., F. J. Brechtel, Y. L. Ma, R. J. Weber, A. Corless, R. C. Flagan, and J. H. Seinfeld (2006), Modeling and characterization of a particle-into-liquid sampler (PILS), *Aerosol Sci. Technol.*, *40*, 396–409, doi:10.1080/02786820600632282.
- Takegawa, N., T. Miyakawa, K. Kawamura, and Y. Kondo (2007), Contribution of selected dicarboxylic and omega-oxocarboxylic acids in ambient aerosol to the m/z 44 signal of an aerodyne aerosol mass spectrometer, *Aerosol Sci. Technol.*, *41*, 418–437, doi:10.1080/02786820701203215.
- Topping, D. O., G. B. McFiggans, and H. Coes (2005), A curved multi-component aerosol hygroscopicity model framework: Part 1. Inorganic compounds, *Atmos. Chem. Phys.*, *5*, 1205–1222.
- Turpin, B., P. Saxena, and E. Andrews (2000), Measuring and simulating particulate organics in the atmosphere: Problems and prospects, *Atmos. Environ.*, *34*, 2983–3013, doi:10.1016/S1352-2310(99)00501-4.
- Twohy, C. H., J. R. Anderson, and P. A. Crozier (2005), Nitrogenated organic aerosols as cloud condensation nuclei, *Geophys. Res. Lett.*, *32*, L19805, doi:10.1029/2005GL023605.
- Ward, J. H. (1963), Hierarchical grouping to optimize an objective function, *J. Am. Stat. Assoc.*, *58*(301), 236–244, doi:10.2307/2282967.
- Weber, R. J., D. Orsini, Y. Daun, Y. N. Lee, P. J. Klotz, and F. Brechtel (2001), A particle-into-liquid collector for rapid measurement of aerosol bulk chemical composition, *Aerosol Sci. Technol.*, *35*, 718–727, doi:10.1080/02786820152546761.
- Zhang, Q., M. R. Alfarra, D. R. Worsnop, J. D. Allan, H. Coe, M. R. Canagaratna, and J. L. Jimenez (2005), Deconvolution and quantification of hydrocarbon-like and oxygenated organic aerosols based on aerosol mass spectrometry, *Environ. Sci. Technol.*, *39*, 4938–4952, doi:10.1021/es0485681.
- Zhang, Q., et al. (2007), Ubiquity and dominance of oxygenated species in organic aerosols in anthropogenically influenced Northern Hemisphere midlatitudes, *Geophys. Res. Lett.*, *34*, L13801, doi:10.1029/2007GL029979.
- T. S. Bates and P. K. Quinn, Pacific Marine Environmental Laboratory, National Oceanic and Atmospheric Administration, 9600 Sand Point Way, NE, Seattle, WA 98115, USA. (tim.s.bates@noaa.gov; patricia.k.quinn@noaa.gov)
- D. S. Covert, Joint Institute for the Study of the Atmospheres and Oceans, University of Washington, 3737 Brooklyn Avenue, NE, Box 355672, Seattle, WA 98195-5672, USA. (dcovert@u.washington.edu)
- L. N. Hawkins, S. Liu, L. M. Russell and S. Takahama, Scripps Institution of Oceanography, University of California, San Diego, 9500 Gilman Drive, Mail Code 0221, La Jolla, CA 92093-0221, USA. (lnhawkins@ucsd.edu; liushang@ucsd.edu; lmrussell@ucsd.edu; stakahama@ucsd.edu)